Empirical Calculation Method for Bypass Leakage in Scroll Compressors

Noriaki ISHII[*1], Takuma TSUJI*[2], Eiji NONOGUCHI[1], Keiko ANAMI[1],
Yuya TERADA[1],Takashi MORIMOTO[3], Charles W. KNISELY[4]

[1] Osaka Electro-Communication University, Osaka, Japan.
ishii@isc.osakac.ac.jp

[2] Mayekawa Mfg. Co., Ltd., Ibaraki, Japan
takuma-tsuji@mayekawa.co.jp

[3] Panasonic Corporation Appliances Company, Shiga, Japan
morimoto.takashi@jp.panasonic.com

[4] Mechanical Engineering Department, Bucknell University, USA
knisely@bucknell.edu

ABSTRACT

This study presents a new idea for an empirical method to calculate the bypass leakage mass flow rate along the tip seal in scroll compressors. A bypass leakage test model was precisely developed to be compatible with a practical scroll compressor with large cooling capacity. Detailed tests of pressure decay in a pressurized vessel due to the bypass leakages were conducted with dry refrigerant gas R410A. The measured pressure decay characteristics were subsequently simulated using the Darcy-Weisbach equation with an empirical friction factor determined in our previous study for the leakage flow through axial clearances. In the present simulations of the measured pressure decay, the complicated flow patterns through bypass clearances were decomposed into two thin representative rectangular cross-section leakage passes, one with the effective mean width and another with the effective mean length. Empirical values of the equivalent pass width and length were determined so that the measured pressure decays are well predicted by the calculations. As a result, the bypass leakage flow rate along the tip seal in scroll compressors can be calculated by a very simple scheme introducing the equivalent pass width of one representative leakage pass with a thin rectangular cross-section.

1. INTRODUCTION

In recent years, scroll compressors have become an increasingly popular choice in many fields, because of their low vibration, low noise and high efficiency. Continued performance enhancement is desired, with improvement in volumetric efficiency as one of the key factors. Major factors affecting the volumetric efficiency are the tangential and radial leakages through the passages between the orbiting and fixed scrolls, especially for small cooling capacity scroll compressors. These leakage flows through the small axial and radial clearances between the orbiting and fixed scrolls have been studied extensively by Ishii *et al.* (1996, 2011) and Oku *et al.* (2005). The pressure decay in the pressurized vessel due to each leakage through the axial and radial clearances was measured using a maximum pressure of 3 MPa for CO2 and 0.6 MPa for R22, and the Darcy-Weisbach equation for incompressible, viscous fluid flow through the thin rectangular cross-section was applied to calculate the leakage mass flow rate, thus simulating the pressure decay characteristics, where the empirical friction factors are determined and plotted on a Moody diagram. As a result, it has been clearly demonstrated that the empirical friction factors for both axial and radial clearance leakage flows take on essentially the same value for both CO2 and R22, despite the significantly different working pressures.

For a low pressure type scroll compressor with large cooling capacity, in contrast to the small capacity compressors, the axial clearance of the scroll compressor becomes relatively large and hence a large leakage loss due to the radial flow through the axial clearance occurs if designed with no countermeasure. In order to eliminate reduce the impact

of this leakage on the volumetric efficiency, tip seals are generally inserted into a tangential slot machined along the end of the scroll wrap. With the installation of tip seals, the radial leakage flow through the relatively large axial clearance can be reduced to a minimum level, but another new leakage flow occurs. It is the so-called "bypass leakage." Bypass leakages appear along the tip seal and has such complicated flow patterns that even the leakage characteristics seems not to be well studied, let alone formulating a method for calculating the bypass leakage mass flow rate (see Youn *et al.,* 2000). The main purpose of this study is to present a new and very simple empirical scheme for calculating the mass flow rate caused by bypass leakages.

In the present study, a new idea is proposed to represent the complicated bypass leakage by a very simple flow model of parallel passages with rectangular cross-section. The complicated flow patterns through bypass clearances are classified into two representative flows through rectangular thin cross-section passes, one with the equivalent width for the radial leakage along the tip seal and the other with the effective mean length for the tangential leakage over the scroll wrap in front of the tip seal. Empirical values of the effective pass mean width and length are so determined such that the measured pressure decays are accurately simulated with calculations. Secondly, a bypass leakage test model is processed precisely, compatible with large-power scroll compressors of about 20 kW class. Two steps of pressure decay tests were conducted in detail, with dry refrigerant gas R410A. The first step was to determine the effective mean length of the rectangular cross-section passage and the second step was to determine the effective mean width. The measured time-dependent curves of pressure decay are simulated by applying the Darcy-Weisbach equation for incompressible and viscous fluid flow, where the empirical friction factor determined in our previous study (Oku et al., 2005) for the leakage flow of dry CO_2 and R22 gas through the axial and radial clearances was applied. Finally, a careful examination of the level of contribution of each representative leakage pass to the resultant leakage was undertaken. Ultimately, the complicated bypass leakage flow can be represented by a single simple leakage flow through a rectangular cross-section passage with an effective mean width empirically determined from the tests presented in this paper

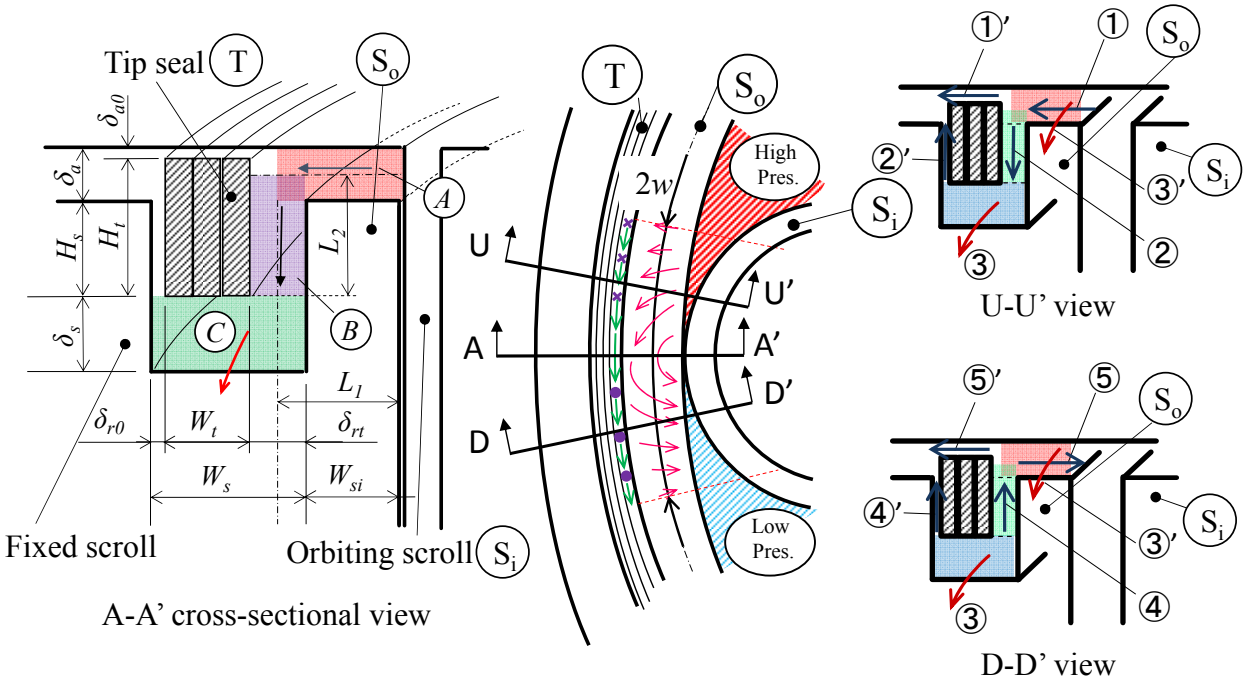

Figure 1 Configuration of bypass leakage flows:
(a) A-A' cross-sectional view for installation of tip seal into slot on scroll wrap; (b) Top view for bypass leakage flow patterns; (c) U-U' cross-sectional view for in-flow from high pressure region to tip-seal slot; (d) D-D' cross-sectional view for out-flow from tip-seal slot to low pressure region.

2. EQUIVALENT LEAKAGE FLOW MODEL WITH PARALLEL PASSAGES WITH RECTANGULAR CROSS-SECTION

2.1 Basic Configuration of Bypass Leakage Flows

The configuration of general installation of the tip seals into a rectangular slot machined on the top of the scroll wrap is shown in Figure 1(a). The right hand side faces a high pressure region and the left hand side faces a low pressure region. The tip seals are pressed against the left hand side wall of the slot and upward onto the orbiting thrust plate, caused by the hydrodynamic effects. However, leakage clearances δ_{rt0} and δ_{a0} still remain behind and above the tip seal, respectively. In the present study, however, these leakages through these clearances are assumed to be negligible when compared with the other leakages. The major bypass leakages occur through the clearance δ_a (leakage region "A") over the front scroll wrap, with the length L_1, the clearance δ_{rt} (leakage region "B") in front of the tip seal, with the length L_2 and the clearance δ_s (leakage region "C") with the width W_s. A top view of the bypass leakage flow patterns is illustrated in Figure 1(b). The flow in the region "A" above the scroll wrap consists of radial and tangential flows. The radial flow (labelled ①) from the high pressure region changes its direction downward in front of the tip seal and flows into the region "B" (labelled ②) and then into the slot under the tip seal; furthermore, the flow changes its direction again in the tangential direction along the tip seal slot indicated in region "C" (labelled ③), as shown in Figure 1(c). The out flow (labelled ③ to ⑤) from the tip seal slot into the low pressure region is the opposite of the in-flow (labelled ① to ③), as explained above, and shown in Figure 1(d). The tangential flow in the region "A" (labelled ③') directly flows from the high pressure region into the low pressure region.

2.2 Equivalent Parallel Rectangular-Cross-Section Passages

The in- and out-flows, labelled ① to ⑤, are classified as a leakage flow Model-1, which can be represented as a leakage flow through a simple thin rectangular cross-sectional passage with the effective mean width and an equivalent length. First, the fundamental idea for the effective mean width is presented in Figure 2, in which the radial in-flow velocity distribution along the tangential direction over the scroll wrap is illustrated. The high pressure region between the outer scroll S_o and the inner scroll S_i forms a wedge, and hence the refrigerant gas is concentrated into the tip of the wedge and then flows out in the radial direction over the outer scroll, thus exhibiting an increase in radial flow velocity as it approaches the contact point of the outer and inner scrolls. This kind of flow may be analyzed with FEM computer calculations, but such a time-consuming method is seldom effective in practical calculations of the volumetric efficiency of scroll compressors under a variety of various operating conditions. A very simple scheme to roughly evaluate this leakage flow, which in turn can afford an accurate calculation of the leakage mass flow rate, is absolutely needed. For this purpose, the concept of "effective mean width", represented by w, is introduced, in which the flow velocity is assumed constant. It is suggested here that the effective mean width naturally depends upon the pressure difference between the high and low pressure regions and its empirical value can be easily determined by leakage tests.

With introduction of the effective mean width w, the in- and out-flows, labelled ① to ⑤, can be represented by a very simple step-like passage with the same effective mean width for all the flow steps, as shown in Figure 3, where the clearance and length of each passage is δ_a and L_1 for the flows ① and ⑤, while δ_{rt} and L_2 are for the flows ② and ④. Here, the Darcy-Weisbach equation is applied to each flow labelled ①, ②, ④ and ⑤:

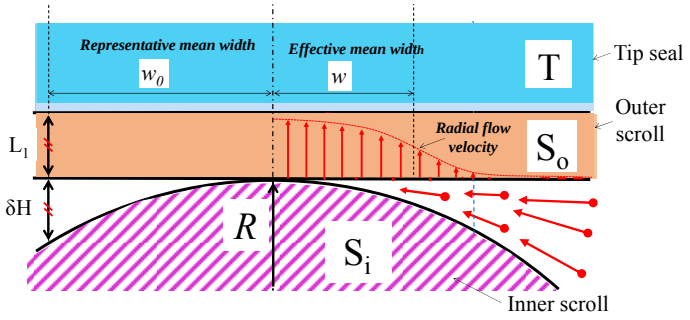

Figure 2 Effective mean width for radial flow over outer scroll (scroll wrap, labelled S_o) and its representative value for non-dimensional form.

$$\frac{P_H - P_{12}}{\rho g} = \lambda \frac{L_1}{2\delta_a} \frac{u_{m1}^2}{2g}, \quad (1)$$

$$\frac{P_{12} - P_s}{\rho g} = \lambda \frac{L_2}{2\delta_{rt}} \cdot \frac{u_{m2}^2}{2g}, \quad (2)$$

$$\frac{P_s - P_{45}}{\rho g} = \lambda \frac{L_2}{2\delta_{rt}} \cdot \frac{u_{m4}^2}{2g}, \quad (3)$$

$$\frac{P_{45} - P_L}{\rho g} = \lambda \frac{L_1}{2\delta_a} \frac{u_{m5}^2}{2g}, \quad (4)$$

where the pressure loss for the flow labelled ③ is disregarded since the clearance height δ_s is generally far larger than δ_a and δ_{rt}. The continuity equations are given by

$$u_{m1}\delta_a w = u_{m2}\delta_{rt} w = u_{m4}\delta_{rt} w = u_{m5}\delta_a w . \quad (5)$$

The summation of each side of the Darcy-Weisbach equations (1) to (4), with consideration of the continuity equation (5), results in the following simple form:

$$\frac{P_H - P_L}{\rho g} = \lambda \frac{l_1}{2\delta_a} \frac{u_{m1}^2}{2g} , \quad (6)$$

where

$$l_1 \equiv 2L_1 + 2L_2\left(\frac{\delta_a}{\delta_{rt}}\right). \quad (7)$$

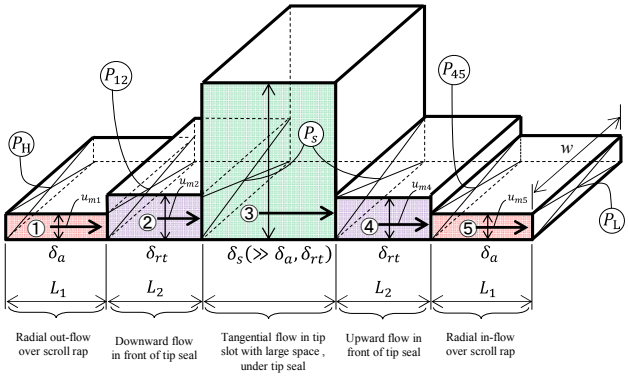

Figure 3 Equivalent steps-like passages with effective width, for flows labelled 1 to 5 of bypass leakage.

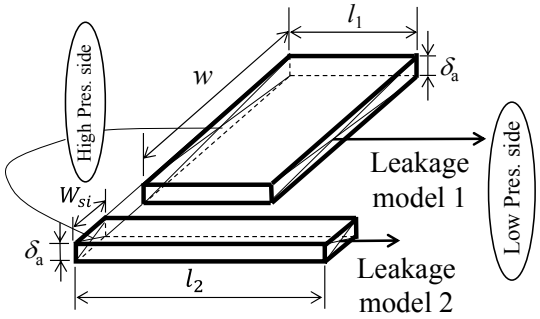

Figure 4 Equivalent flow model of parallel rectangular-cross-section passage, consisted of Model 1 and Model 2, for bypass leakages.

Equation (6) represents the reduction of the step-like passage, shown in Figure 3, to the simplest rectangular cross-section passage, as shown by the leakage Model-1 in Figure 4. The clearance height is δ_a and the equivalent length are l_1, is defined by Equation (7).

One additional leakage exists in addition to this leakage Model-1. This additional leakage is the tangential flow over the scroll wrap, labelled 3', as shown in Figures 1(c) and (d). This tangential flow through the minimal rectangular cross-section with the clearance height δ_a and the width W_{si} can be simply represented by a flow through the rectangular cross-section passage with the effective mean length l_2, as shown by the leakage Model-2 in Figure 4. It is suggested that the empirical value of the effective mean length l_2 can be easily determined by leakage tests. The Darcy-Weisbach equation for this leakage Model-2 is given by

$$\frac{P_H - P_L}{\rho g} = \lambda \frac{l_2}{2\delta_a} \frac{u_{m2}^2}{2g} . \quad (8)$$

3. LEAKAGE TESTS AND DETERMINATION OF EFFECTIVE MEAN LENGTH AND WIDTH OF PARALLEL RECTANGULAR CROSS-SECTION PASSAGES

3.1 Leakage Test Set-Up

Photos of the present leakage test set-up are shown in Figure 5, in which the most important plate S_o is sandwiched between the upper and lower plates. The high pressure region of P_H on the left is connected to the pressurized tank with a volume of 860 cm^3 and the low pressure region of P_S on the right to a refrigerant recovery tank with

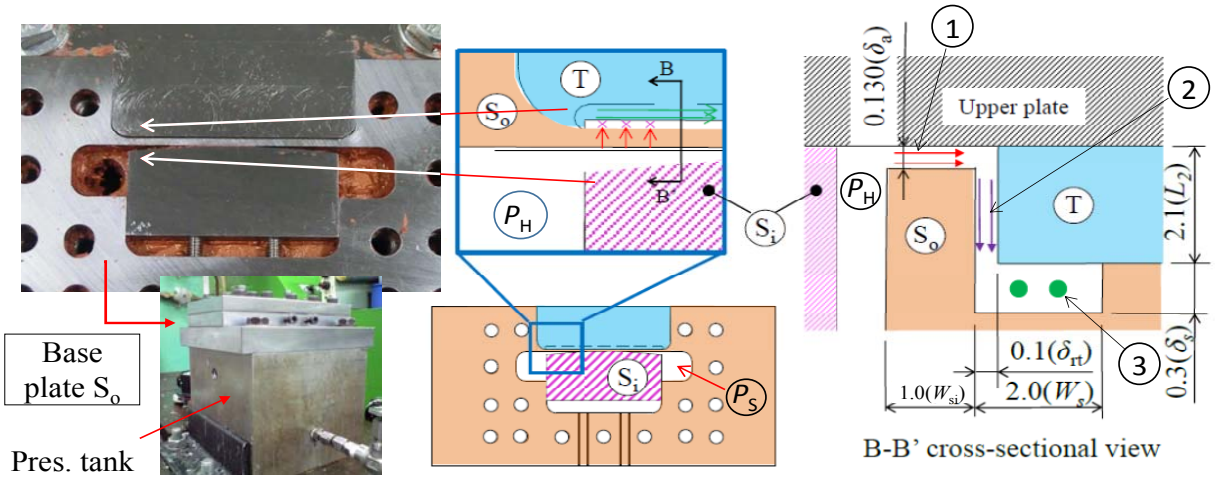

Figure 5 Configuration of lubrication test set-up.

atmospheric pressure, through a release valve. The linear tip seal slot is precisely machined on the base plate S_o, as shown in the B-B' cross-section shown right-most in Figure 5. The width W_s is 2.0 mm and the height is 2.27 mm on the left side and 0.3 mm (δ_s) on the right side, on which the tip seal plate with the height of 2.1 mm (L_2) is mounted so that the axial clearance height δ_a of 0.130 mm is achieved over the left side of the slot. The radial clearance of 0.1 mm is kept between the slot on the left side and the tip seal plate side. The outer scroll S_o has a horizontal length of 70 mm, while the inner scroll S_i with the same length, is shaded in pink, and has a radius R of 30 mm.

Table 1 Major specifications for bypass leakage tests.

Equivalent passage length l_1 [mm]	7.56
Pass length L_1 [mm]	1.05
Pass length L_2 [mm]	2.1
High pressure P_H [MPa]	0.4 ~ 1.2
Low pressure P_S [MPa]	0.1
Inner scroll radius R [mm]	30
Slot width W_s [mm]	2.0
Width W_{si} [mm]	1.0
Axial clearance δ_a [μm]	130
Radial clearance δrt [μm]	100
Slot heghit δs [μm]	300

The refrigerant gas R410A in the high pressure region with P_H flows through the axial clearance over the left side of the slot S_o, labelled ①, and flows downward in front of the tip seal plate left side, labelled ②, and flows tangentially along the tip seal slot, labelled with ③, and then in the opposite direction toward the low pressure region with P_S. The major specifications for the present leakage tests are listed in Table 1. The equivalent passage length l_1 of Model-1 is 7.56 mm, calculated from the defining Equation (7).

3.2 Pressure Decay Test Results and Determination of Effective Mean Width for Leakage Mode-1 and Effective Mean Length for Leakage Model-2

The test itself is very simple and easy to conduct. Initially, the release valve is closed to pull the air from the inside of the whole system with a vacuum pump and then the system is charged with refrigerant gas R410A. The release valve is opened as quickly as possible and the pressure decay in the pressurized tank, due to gas leakage, is measured until the pressure in the high pressure tank decreases to atmospheric pressure. Careful attention was paid to seal perfectly the contact surfaces between the parts, with a fluid gasket, so that the bypass passages are not sealed.

The initial high pressure in the tank, P_H, was increased from 0.4 MPa to 1.2 MPa in steps of 0.1 MPa, relative to the atmospheric low pressure P_S of 0.1 MPa. Thus, the pressure difference Δp changed from 0.3 to 1.1 MPa. Test results of the pressure decay due to bypass leakage, detected with a pressure transducer (JTEKT, PMS-5M), are shown by a solid line (black) in Figure 6. Figure 6(a) represents the pressure decay due to the resultant leakage for Models -1&2, while Figure 6(b) represents the pressure decay due to a leakage only for Model-2, where the leakage passages for Model-1 were completely and carefully sealed. The leakage cross-section area for Model-2 is very small compared

with that for Model-1 and, hence, the pressure decay shown in Figure 6(b) takes far more time the pressure decay shown in Figure 6(a) for Models-1&2.

The empirical friction factor λ in the Darcy-Weisbach equation was empirically determined by Ishii, et al. (1996, 2011) and Oku et al., (2005). It can be represented by a Nikuradse-style formula

$$\lambda = 0.0032 + 1.5\,\mathrm{Re}^{-0.35}, \quad \text{where the Reynolds number is} \quad \mathrm{Re} \equiv 2\delta_a \rho u_m / \mu, \tag{9}$$

which is a result for the refrigerant R22 and is shown on the Moody diagram in Figure 7. With the introduction of this empirical friction factor into Equations (6) and (8), the leakage flow velocity u_{m1} and u_{m2} can be calculated and thus the mass flow rate $\dot{m}$ can be calculated by

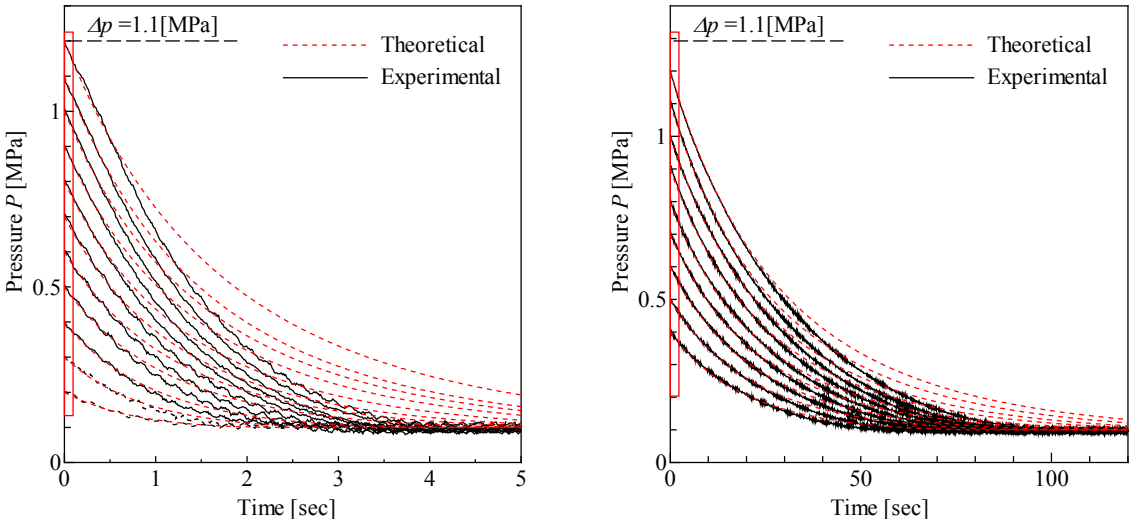

(a) Pressure decay for Model-1&2. (b) Pressure decay for Model-2.

Figure 6 Pressure decay test results and its theoretical simulation for determination of effective mean width w for Model-1 and effective mean length l_2 for Model-2.

$$\begin{aligned} \dot{m} &= \rho\delta_a w u_{m1} \quad \text{for Model-1} \\ \text{or} \quad &\rho\delta_a W_{si} u_{m2} \quad \text{for Model-2} \end{aligned} \tag{10}$$

where the density ρ can be calculated by

$$\rho = \rho_0 \left(P / P_0\right)^{1/n}. \tag{11}$$

The initial pressure and density are represented by P_0 and ρ_0, respectively. The residual refrigerant mass in the high pressure chamber, G, can be calculated by subtracting the total leakage mass from the initial refrigerant mass G_0:

$$G = G_0 - \int_0^t \dot{m} dt \tag{12}$$

Finally, assuming a polytropic process with exponent n, the pressure decay ΔP in the high pressure chamber over a small time Δt can be calculated:

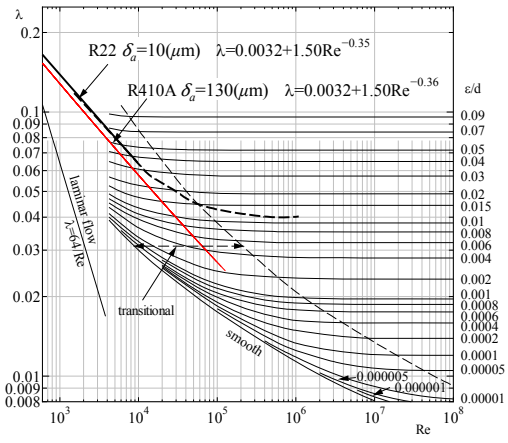

Figure 7 Empirical friction factor on Moody diagram.

$$\Delta P = \frac{P_0}{G_0^{\,n}} n G^{n-1} \dot{m} \Delta t \,. \qquad (13)$$

Calculated results for the pressure decay are shown by a dashed line (red) in Figure 6. During the initial time step, the pressure decay for Model-2, shown in Figure 6(b), was theoretically simulated so that the theoretical curve predicts well the measured pressure decay in the time region immediately after the measurement started, where the effective passage length l_2 was determined first. Similar simulations were conducted for all measured pressure decays and the determined empirical data of l_2 is plotted over the pressure difference ΔP, as shown in Figure 8, exhibiting a linear increase from about 3 mm to about 8 mm, with increasing initial pressure difference ΔP from 0.1 to 1.1 MPa. Adopting this empirical value for l_2 in the next step, the pressure decay for Model-1&2, shown in Figure 6(a) was theoretically simulated so that the theoretical curve again predicted the measured pressure decay over the time increment immediately after the measurement started, where the effective passage width w was determined. The empirical data of w is plotted over the pressure difference ΔP, as shown in Figure 8, exhibiting a quadratic-like decrease from about 22 to about 8 mm, with increasing initial pressure difference ΔP.

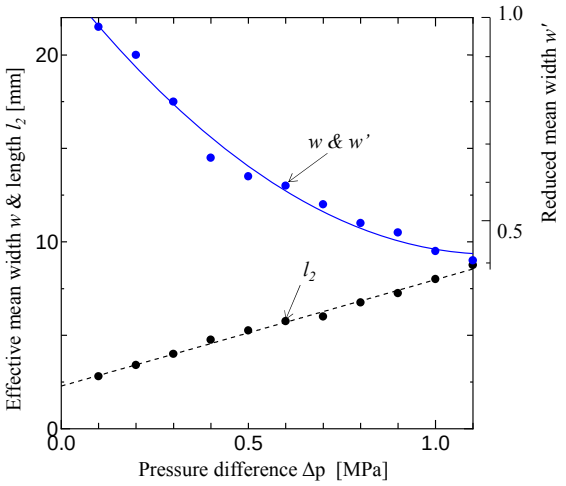

Figure 8 Effective mean width w and length, determined from pressure decay tests.

4. CONFIRMATION OF EMPIRICAL CALCULATION METHOD FOR ITS VALIDITY

In the theoretical simulations shown in Figure 6(a), the effective mean width w and length l_2 were kept at a value determined from the data at the time immediately after the measurement started, for the whole time duration over which the measurements were made. For this reason, it is suggested, the theoretically simulated curves exhibit substantial differences from the measured ones, which increases as time passes.

As a result, the theoretical calculations were conducted again for the whole time duration, adopting the empirical data of w and l_2, shown in Figure 8, depending upon the pressure P. Re-calculation results are all shown by a dashed line (red) again in Figure 9, where the friction factor λ was adjusted slightly to provide a best fit curve, given by

$$\lambda = 0.0032 + 1.5\,\mathrm{Re}^{-0.36}, \qquad (14)$$

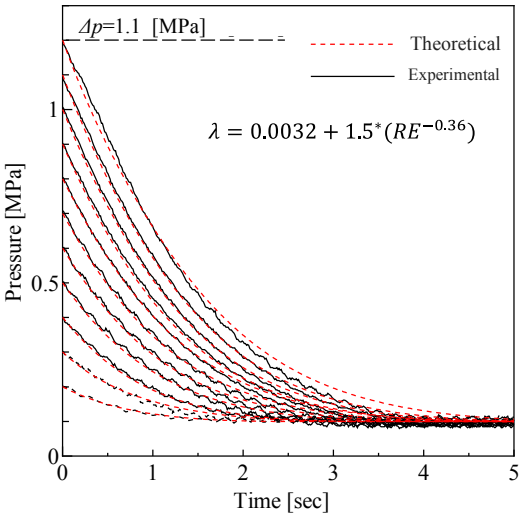

Figure 9 Theoretical simulation of pressure decay for Models-1&2, compared with test results.

which is shown by a red solid line in Figure 7, for comparison with the previous result for the refrigerant R22 and for the radial clearance δ_a of 10 μm. The present empirical result is for the refrigerant R410A and the clearance height of 130 μm which is more than 10 times larger than that for the previous tests. In spite of different refrigerants and different clearances, the empirical friction factor does not change much at all.

The calculated results shown by the red dashed lines are in a close agreement with the test results (solid black lines) for the measured time duration. This drastic improvement from the comparison shown in Figure 6(a) confirms the validity of the present idea of representing the complicated bypass leakage flows by the very simplified flows through the parallel rectangular cross-section passages.

In addition, the effective mean width w is normalized by the representative tangential length w_0, presented in Figure 3, in which special attention is paid to the distance δH between the outer and inner scrolls, increasing with distance from the contact point. The representative mean length w_0 is the horizontal (tangential) length from the contact point where the clearance height δH becomes equal to the outer scroll thickness L_1, which takes on a value of 22.0 mm for the present test set-up. Thus, a normalized quantity, the so-called "reduced mean width w'," is shown on the right hand scale in Figure 8. The reduced mean width $w'(\equiv w / w_0)$ is close to 1.0 when the pressure difference is small, and gradually decreases to about 0.4 at the maximum pressure difference of 1.1 MPa. This result indicate that the present selection of the representative mean width w_0 was physically correct. It is suggested that the empirical result

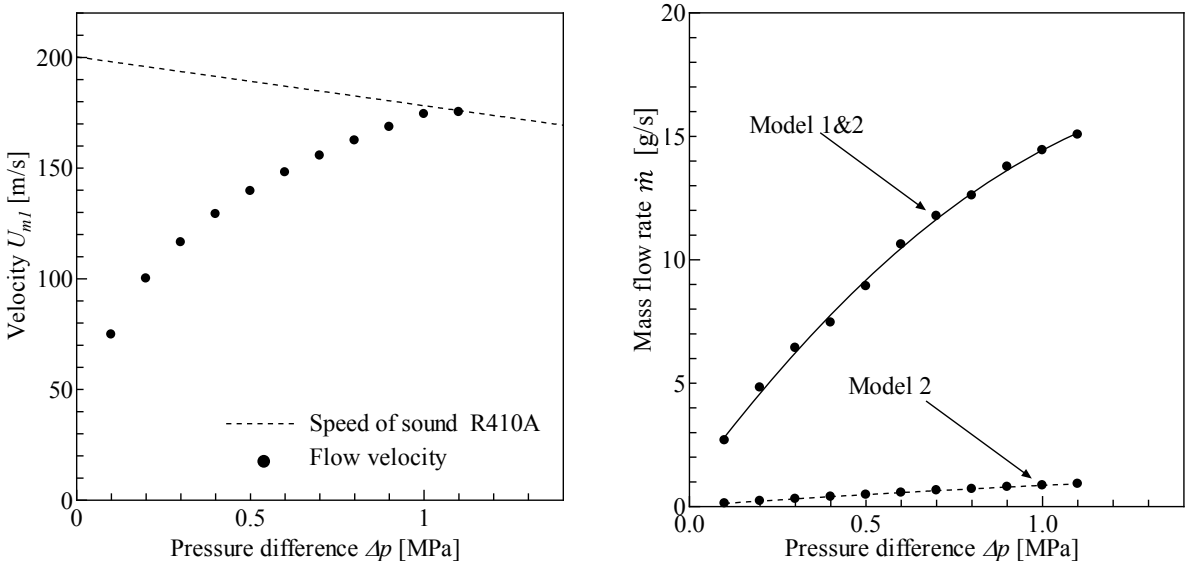

(a) Leakage flow velocity u_{m1}. (b) Mass flow rate $\dot{m}$.

Figure 10 Empirical data of leakage flow velocity u_{m1} and mass flow rate $\dot{m}$ vs. pressure difference ΔP.

of reduced effective mean width, presented in Figure 8, can be applied to all cases with different radii for the outer and inner scrolls, in calculations of bypass leakages in scroll compressors.

5. LEAKAGE MASS FLOW RATE AND DOMINANT LEAKAGE FLOW MODEL

In the process of the pressure decay simulations, the leakage flow velocity u_{m1} and mass flow rate $\dot{m}$ have been calculated, as shown in Figure 10, over the pressure difference Δp. All leakage velocity data, except for the single value at Δp = 1.1, are lower than the sound velocity for R410A, shown by the dashed line in Figure 10(a). For this reason the working fluid of refrigerant gas can be treated as incompressible, for the leakage flow through very thin passages. Only one calculated flow velocity data point at Δp =1.1 exceeded the sound velocity. In this case, the choking flow through the passage would force the velocity to be the speed of sound at Δp =1.1.

All data of the mass flow rate $\dot{m}$ align well along the solid and dashed lines, respectively, as shown in Figure 10(b). The upper solid line is for the leakage by Model-1&2, and the lower dashed line is for Mode-2 which is about 5%

relative to that for Model-1&2. The leakage by Model-1 is far dominant. From this result, one may disregard the leakage effect for Model-2, in simulation of bypass leakage for determining the volumetric efficiency of scroll compressors, if 5% error is permitted.

6. CONCLUSIONS

In the present study, the hypothesized treatment of complicated bypass leakage in scroll compressors using a very simple flow model was validated. In the flow model parallel rectangular cross-section passages, classified into Model-1 with the effective mean width for the radial leakage along the tip seal and Model-2 with the effective mean length for the tangential leakage over the scroll wrap in front of the tip seal are used to simulate the bypass leakage flow. The effective mean width and the effective mean length were determined by very simple and easily conducted pressure decay tests, where the measured pressure decays were all successfully simulated by very simple theoretical calculations, based on the Darcy-Weisbach equation for incompressible viscous fluid flow. Furthermore, the level of contribution to the resultant leakage is examined to conclude that the leakage by Model-1 is by far the dominant effect and the complicated bypass leakage can be calculated by just one rectangular cross-section passage represented by Model-1, if an error of about 5% is permissible. Finally, the effective mean width for Model-1 was normalized with the representative tangential length from the contact point of the outer and inner scrolls, where the distance between the outer and inner scrolls becomes equal to the thickness of outer scroll wrap in front of the tip seal. In this way, the reduced effective mean width was formulated, and the present scheme for empirically calculating the complicated bypass leakage was generalized for possible application to all cases of scroll contact area geometry.

The present study was motivated through possible developments of super large scroll compressors with shaft power more than 1000 kW, where the bypass leakage effect on the volumetric efficiency was one unknown factor for the authors. The present scheme for evaluating the complicated bypass leakage will be applied to predict the possible high volumetric efficiency of super large scroll compressors.

NOMENCLATURE

G, G_0	: Refrigerant mass	[kg]	Re	: Reynolds number	[-]
g	: Acc. of Gravity	[m/s^2]	t	: Time	[s]
L_1, L_2	: Length	[m]	$u_{m1}, u_{m2}, u_{m3}, u_{m4}$	: Mean velocity	[m/s]
l_1, l_2	: Equivalent length	[m]	W_s	: Width	[m]
$\dot{m}$	: Mass flow rate	[kg/s]	δ_a, δ_{rt}, δ_{a0}, δ_{r0}	: Clearance	[m]
n	: Polytropic index	[-]	λ	: Friction factor	[-]
$P_H, P_s, P_L, P_{12}, P_{45}$	: Pressure	[Pa]	ρ	: Density	[kg/m^3]

REFERENCES

Ishii, N., Bird, K., Sano, K., Oono, M. Iwamura, S. & Otokura, T., 1996, Refrigerant Leakage Flow Evaluation for Scroll Compressors, *International Compressor Engineering Conference at Purdue*, pp.633-638.

Ishii, N., Tsuji, T., Oku, T., Anami, K. Matsui, A. & Knisely, C., 2011, Exploration of Optimal Efficiency Super-Large Cooling Capacity Scroll Compressors for Air Conditioners, *International Conference of ICR at Prague*, ID.: 945.

Oku, T., Anami, K., Ishii, N., Knisely, C., Yasuda, K., Sawai, K. Sano, K. & Morimoto, T., 2005, Gas Leakage in CO2 and R22 Scroll Compressors and Its Use in Simulations of Optimal Performance, *International Compressor Engineering Conference at Purdue*.

Youn, Y., Cho, N., Lee, B. & Man, M., 2000, The Characteristics of Tip Leakage in Scroll Compressors for Air-Conditioners, *International Compressor Engineering Conference at Purdue*, p.797.

ACKNOWLEDGEMENT

This study was initiated through research collaborations with Danfoss Commercial Compressors. The authors express their sincere gratitude to Danfoss people for their kind regards. The authors extend their sincere gratitude to Mr. Isao Tasaka, Director, Air-Conditioning and Cold Chain Development Center, Corporate Engineering Division, and Mr. Akio Kozaki, Director, Refrigeration and Air-Conditioning Devices Business Division, Appliances Company, Panasonic Co., Ltd., for their cooperation in carrying out this work and their permission to publish this study.